Stochastic Modeling for Uncertainty Analysis and Multiobjective Optimization of IGCC System with Single-Stage Coal Gasification

ARTICLE *in* INDUSTRIAL & ENGINEERING CHEMISTRY RESEARCH · NOVEMBER 2010

Impact Factor: 2.59 · DOI: 10.1021/ie101355x

2 AUTHORS:

Yogendra Shastri
Indian Institute of Technology Bombay
64 PUBLICATIONS **291** CITATIONS
SEE PROFILE

Urmila Diwekar
University of Illinois at Chicago
124 PUBLICATIONS **1,512** CITATIONS
SEE PROFILE

I&EC research
Industrial & Engineering Chemistry Research

ARTICLE

pubs.acs.org/IECR

Stochastic Modeling for Uncertainty Analysis and Multiobjective Optimization of IGCC System with Single-Stage Coal Gasification

Yogendra Shastri[†] and Urmila Diwekar*

Center for Uncertain Systems: Tools for Optimization and Management, Vishwamitra Research Institute, 368 56th Street, Clarendon Hill, Illinois 60514, United States

ABSTRACT: Integrated Gasification Combined Cycle (IGCC) system using coal gasification is an important component of future energy alternatives. Consequently, understanding the system operation and optimizing it in the presence of uncertain operating conditions is important. Moreover, since gasification is the most important component of the system, it is particularly critical to understand the impact of uncertainty in gasification operation on the IGCC system. This article presents research conducted to achieve these objectives. The work initially focuses on developing a computational fluid dynamics (CFD) model for the single-stage coal gasifier, which is a part of the IGCC system. The impact of varying coal composition on the gasifier operations is determined from the CFD simulations. The stochastic CFD simulation results are then compared with those for an approximate gasifier model developed in ASPEN Plus as a part of the IGCC model to characterize and quantify the gasifier operation uncertainty. The CAPE-OPEN compliant stochastic simulation capability is also used to perform deterministic and stochastic multiobjective optimization of the IGCC system. This is based on the Parameter Space Investigation (PSI) method of multiobjective optimization useful for nonconvex nonlinear surface. Stochastic modeling is also useful for identifying important decision variables for such surfaces using Partial Rank Correlation Coefficients (PRCC).

1. INTRODUCTION

Integrated Gasification Combined Cycle (IGCC) system is a critical component of future sustainable energy alternatives.[1−4] The important advantages of the IGCC system as compared to conventional power generation systems using pulverized coal are higher thermal efficiency and lower emissions.[5,6] Consequently, there has been a significant focus on science and engineering aspects of the IGCC system as well as various innovations within the system.[6−11] Coal is an abundantly available and cheap source of fossil energy in various parts of the world. However, there are serious concerns related to the greenhouse gas emissions associated with the use of coal. Given this, IGCC system using coal gasification presents a sustainable option for the use of coal for power generation.[12−14] The operation of the IGCC system, however, is subject to various uncertainties, including the process input parameters as well as the operating parameters. Coal gasification is an important component of the IGCC system. Consequently, the impact of coal gasifier operations and the uncertainties associated with coal gasification need to be understood and quantified. The results can then be used for optimizing the performance of the IGCC system.

The scope of this work is to use the CAPE-OPEN compliant stochastic modeling capability[15] to conduct a comprehensive uncertainty analysis of the Integrated Gasification Combined Cycle (IGCC) system based on single-stage downflow coal gasifier. To achieve this objective, a CFD model for the single-stage downflow gasifier is developed in FLUENT. Then, uncertainties in the IGCC process that will be encountered in real systems and impact the performance of the whole system are identified and quantified. Stochastic simulations of the gasifier CFD model in FLUENT are conducted for uncertainty quantification of the detailed gasifier model. Then, multiobjective optimization using the CAPE-OPEN capability on the Aspen Plus IGCC system is carried out to determine the Pareto surface that can help in the operation of the system.

The rest of the article is arranged as follows. Section 2 provides an overview of Integrated Gasification Combined Cycle (IGCC) system using a single-stage gasifier. Section 3 describes the CFD modeling of the single-stage downflow gasifier and presents the simulation results for the basic model. Section 4 discusses the uncertainty characterization and quantification for the gasifier model and presents results for the stochastic simulations of FLUENT model. Section 5 presents the results for deterministic and stochastic multiobjective optimization of the IGCC system using stochastic simulation results for selected decision variables. The article ends with conclusions in section 6.

2. INTEGRATED GASIFICATION COMBINED CYCLE (IGCC) SYSTEM

Integrated Gasification Combined Cycle (IGCC) technology is increasingly important in the world energy market, where low-cost opportunity feedstocks such as coal, heavy oils, and pet coke are the fuels of choice. IGCC technology produces low-cost electricity while meeting strict environmental regulations. There are primarily two important types of gasification technologies commercially available, namely, two-stage upflow entrained gasifier, and single-stage downflow entrained gasifier. This work

Special Issue: Puigjaner Issue

Received: June 25, 2010
Accepted: November 2, 2010
Revised: October 27, 2010
Published: November 22, 2010

dx.doi.org/10.1021/ie101355x | *Ind. Eng. Chem. Res.* 2011, 50, 4879–4892

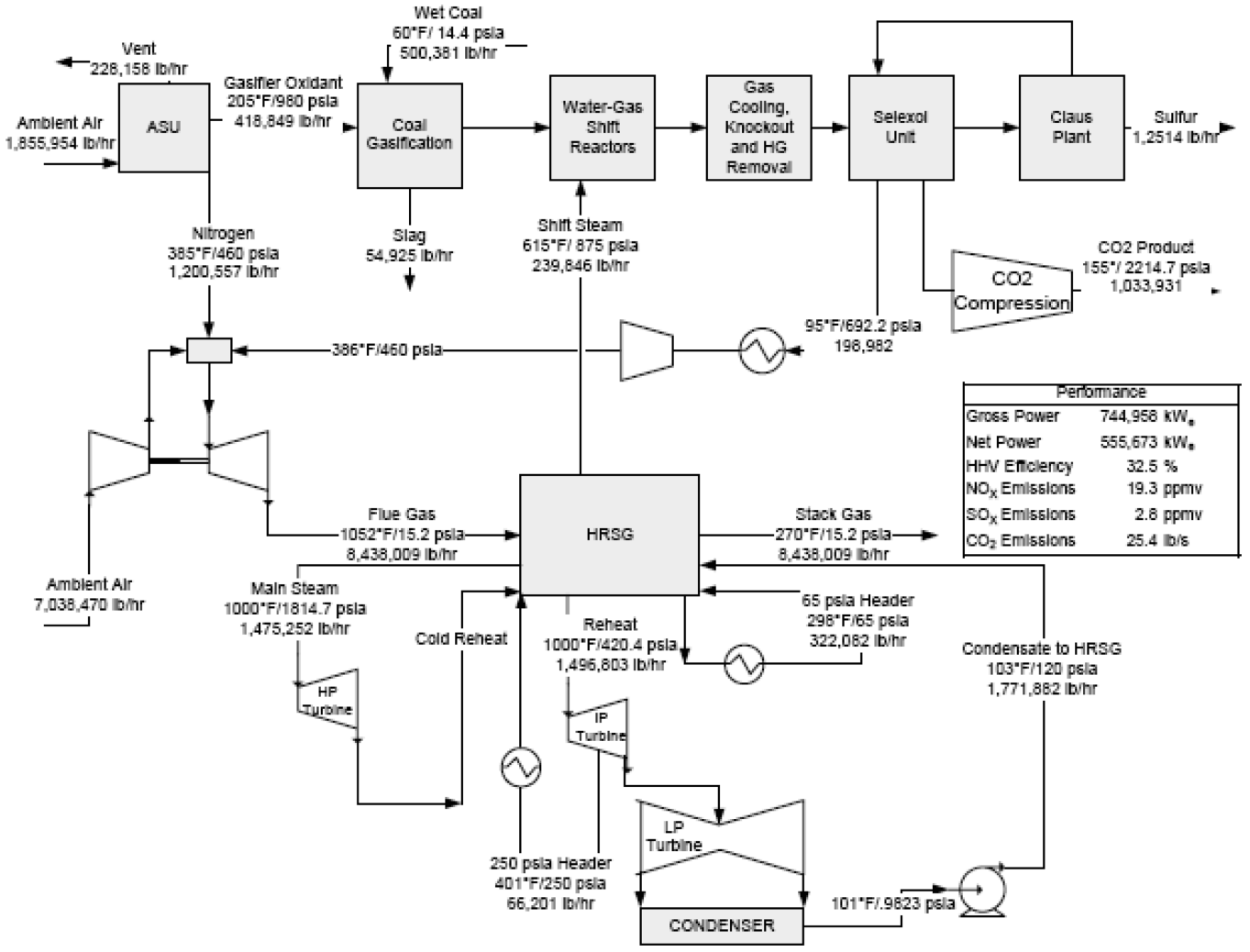

Figure 1. Integrated Gasification Combined Cycle (IGCC) flowsheet.

analyzes the IGCC system incorporating a single-stage downflow gasifier.

Figure 1 shows the IGCC system flowsheet that is used in the current work.[16] The system is based on the General Electric (GE) energy gasifier and two advanced F-class gas turbines partially integrated with an elevated pressure air separation unit (ASU). Syngas desulfurization is provided by a Selexol acid gas removal (AGR) system and a two-bed Claus Unit with tail gas recycle to Selexol. Ninety-five percent CO_2 capture is accomplished in the Selexol system, and the product is compressed to 15.168 MPa (2200 psig). A brief description of the flowsheet is given below. Please refer to ref 16 for further details.

Coal is supplied to the gasifier where it is partially oxidized under pressure of about 223 MPa (56 atm). The plant uses oxygen (with traces of argon and nitrogen) as oxidant. The ASU is responsible for providing the gasifier with 95% oxygen as the gasification oxidant. Slurry water is added to the coal constituents as required to create the coal slurry mixture by design specification. The mixture is set to be 66% solids by weight. The gasifier is set to operate at 1315.5 °C (2400 °F) and 5.6 MPa (814.7 psia) according to the vendor specification. The high temperatures ensure that the noncombustible ash from coal is converted into a liquid slag with low viscosity which easily flows out of the gasifier. Hot raw fuel gas exits the gasifier at approximately 1315 °C/5.6 MPa (2400 °F/814.7 psia). The fuel gas and residual char leaving the cyclone are cooled to 593 °C (1100 °F) raising high-pressure steam in a radiant water-tube boiler. After the radiant cooling, the syngas passes through a quench, where adiabatic operation of the syngas quench cooling cools the syngas down to 210 °C (410 °F). The quench bottoms are then sent to a slag separator and process gas splitter, which completely remove slag and ash, and separate process gas and leftover quench water. The process gas goes back to the syngas stream and the leftover quench, or blackwater, is scrubbed. Steam is added to the syngas exiting the quench system. This sets the H_2O/CO ratio equal to 2 before the water gas shift reactions.

The water gas shift reactions occur in three reactors, with cooling between each. Each of the water gas shift reactors converts approximately 80% of the CO in the feed to CO_2. Over 95% of the COS present in the syngas is also converted to H_2S in the reactors. The cooling between each reactor maintains a reactor inlet temperature of 232 °C (450 °F). Syngas cooling and knockout is accomplished in three stages in an attempt to maximize heat recovery while meeting the temperature demands of downstream systems. After the cooling, the syngas goes through NH_3 conditioning to remove any NH_3 in the stream. The syngas, having been cooled, is sent to the selexol reactor. The feed is separated into three streams: a hydrogen-rich outlet that is

sent to the gas turbine, a CO_2-rich bottoms stream to be compressed for CO_2 capture, and a sulfur-rich stream to be sent to the Claus plant. The Claus reactor is a two-stage reactor and is responsible for removing sulfur compounds from the gas stream. Prior to entering the catalytic reactors, the Claus reactor effluent enters the waste heat boiler where S_2 is converted to S_6 and S_8. Medium pressure (MP) steam is produced from the heat liberated from this reaction. After heating the effluent to 232 °C (450 °F), the tail gas is fed to the tail gas hydrogenation reactor. The condensate is then removed in the tail gas cooler. The effluent from the tail gas cooler goes through a multistage compressor. The tail gas is compressed from 0.128 MPa (18.6 psia) up to 5.35 MPa (776 psia) and recycled back to the selexol reactor.

The gas turbine consists of a syngas heater, air compressor, combustor, and three stages of expansion and cooling, with the appropriate mixers and splitters. The steam turbine consists of an HP section, an IP section, and an LP section, all connected to the generator by a common shaft. Main steam from the heat recovery steam generator (HRSG) and syngas cooler is combined in a header, and then passes through the stop valves and control valves and enters the turbine at 12.4 MPa/537 °C (1800 psig/1000 °F). The steam initially enters the turbine in the high-pressure span, flows through the turbine, and returns to the HRSG for reheating. The reheat steam flows through the reheat stop valves and intercept valves, and enters the IP turbine section at 2.79 MPa/537 °C (405 psig/1000 °F). After passing through the IP section, the steam enters a crossover pipe which transports the steam to the LP section. The steam enters the crossover heater and flows through the LP section, exhausting downward into the condenser at 6.77 kPa (0.9823 psia). The heat recovery steam generator (HRSG) is a horizontal gas flow, drum-type, multipressure design that is matched to the characteristics of the gas turbine exhaust gas. The CO_2 compression section is responsible for compressing CO_2 for capture and sequestration. Aspen Plus model for the IGCC system has been developed by the Department of Energy to conduct system level analysis of the process. The Aspen Plus modeling details (including the modeling approximations and configuration) is explained in ref 16 and not discussed here for the sake of brevity.

3. GASIFIER CFD MODEL DEVELOPMENT

The gasifier is an important operating unit of the IGCC system, and the overall performance of the gasifier (such as efficiency and availability) has a significant impact on the performance of the whole IGCC system. Consequently, the primary focus of uncertainty analysis in this work is on the gasifier, as mentioned in the introduction. The Aspen Plus flowsheet described in the previous section models the gasifier as a reactor and uses the Gibbs Free Energy Minimization method to predict the syngas combustion equilibrium conditions. A computational fluid dynamics (CFD) model, however, is more detailed and allows one to conduct a more accurate analysis of the gasifier performance. Hence the initial task was to develop a CFD model for the single-stage gasifier, and this work used FLUENT to develop the CFD model.

Gasifiers can broadly be classified into three main categories depending on the flow characteristics inside, namely, moving bed, fluidized bed, and entrained flow. Considerable information on the modeling of various types of gasifiers using different approaches can be found in literature.[17−21] The gasifier in the IGCC system considered in this work is a single-stage downflow gasifier. Reaction Engineering International (REI) has conducted various studies on single-stage gasifier using a proprietary CFD simulator GLACIER.[22−24] The overall configuration of the single-stage gasifier includes an inlet at the top of the gasifier and a single outlet that is used to collect syngas as well as molten slag. There is a quench section at the exit of the gasifier which is used to quench the raw syngas produced in the gasifier. Since the quench section is separately modeled in the Aspen Plus flowsheet (as explained in the previous section), it was ignored in the CFD model of the gasifier. Two major steps toward the modeling analysis include:

- Gasifier geometry and FLUENT model setup
- FLUENT model simulation These steps are explained in the following sections.

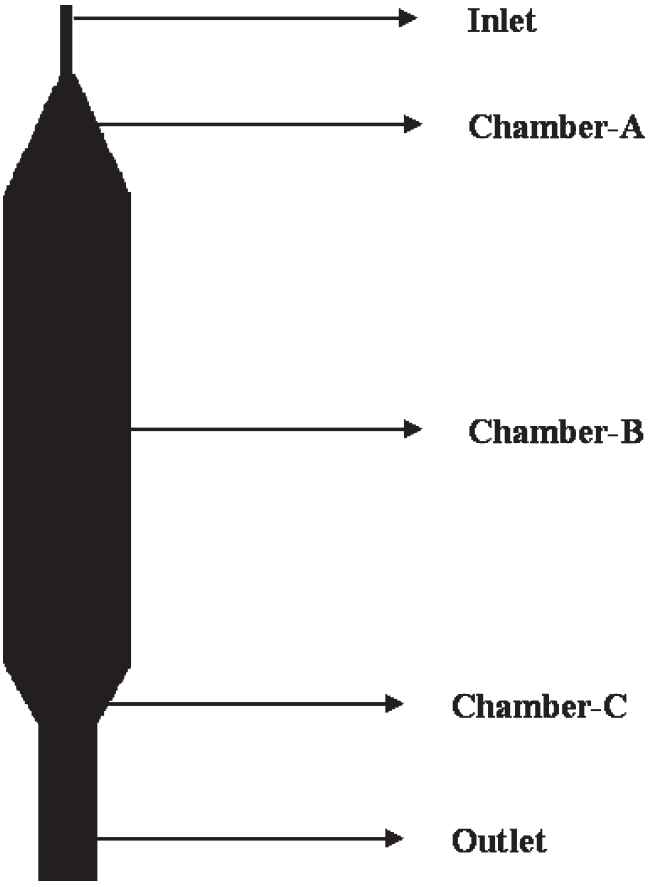

Figure 2. Single-state downflow gasifier geometry.

3.1. Gasifier Geometry and FLUENT Model Setup. The downflow gasifier geometry was finalized based on the literature review as well as the studies conducted in refs 22−24. Figure 2 shows the shape of the gasifier. This geometry also incorporated rigorous heat transfer calculations to compute the refractory lining thickness and the interior geometry of the gasifier. The exact dimensions for the gasifier were as follows:

- Inlet: radius 0.08 m; height 1.0 m; volume 0.02 m^3
- Chamber-A: radius-1 0.08 m; radius-2 0.894 m; height 1.768 m; volume 1.6157 m^3
- Chamber-B: radius 0.894 m; height 6.62 m; volume 16.537 m^3
- Chamber-C: radius-1 0.4 m; radius-2 0.894 m; height 0.864 m; volume 1.1854 m^3

dx.doi.org/10.1021/ie101355x |Ind. Eng. Chem. Res. 2011, 50, 4879–4892

Table 1. Proximate Analysis of Coal

component	percentage on mass basis
fixed carbon	49.71
ash	10.90
volatile matter	29.66
moisture	10.05

Table 2. Ultimate Analysis of Coal

component	percentage on mass basis
carbon	71.72
hydrogen	5.06
nitrogen	1.74
sulfur	2.82
oxygen	7.75
other	10.91

Table 3. Gasifier Exit Gas Composition (Percentage on Molar Basis)

component	percentage on molar basis
H_2O	15.22
argon	0.746
CO_2	14.49
O_2	1.19×10^{-22}
N_2	0.0
CH_4	1.047×10^{-9}
CO	37.15
H_2	31.57
H_2S	0.803
NH_3	0.00

- Outlet: radius 0.4 m; height 2.55 m; volume 1.275 m^3
- Total volume 20.634 m^3

Once the geometry was finalized, the CFD model was set up in FLUENT. The details pertaining to the CFD model setup are the following:

- The coal composition and analysis data (proximate and ultimate analysis) used to simulate the ASPEN Plus IGCC flowsheet were used for the CFD simulation.
- Tables 1 and 2 report the proximate and ultimate analysis values for the coal.
- The total flow rates for coal, slurry water, and oxidant used in the ASPEN Plus simulation were used. The ASPEN plus flowsheet modeled the IGCC system with two gasifiers operating in a parallel configuration. Hence, while calculating the input stream flowrates for the CFD model, the values reported in ASPEN flowsheet were halved.
- All simulations were performed for the actual flow rates (i.e., test simulations for smaller flow rates were not performed). The inlet conditions (temperature and pressure) and the gasifier operating conditions also corresponded to the ASPEN Plus flowsheet.
- The coal particles in the gasifier were modeled as discrete phase. The dynamics of coal (such as transport and reactions) were described by a user defined function (UDF) which modeled coal as a discrete phase. The UDF was compiled to the FLUENT model and was periodically accessed to model coal dynamics. Details about the UDF development can be found in ref 21.
- The gasifier model was developed using GAMBIT and meshed using 14406 nodes and 13104 tetrahedral cells (with Cooper mesh scheme). The mesh was exported to FLUENT to develop the CFD model.

Table 4. Gasifier Exit Stream Mass Flow Rate and Temperature

exit stream property	value
exit gas flow rate (kg/s)	66.926
exit gas temperature (K)	2425.48
slag flow rate (kg/s)	3.438
slag temperature (K)	2426.63

3.2. Model Simulation Results. Forty thousand iterations for the FLUENT model were required for the model to converge. The discrete phase model was simulated after 50 iterations of the continuous phase and about 80 000 particles of the discrete phase were tracked during the simulation. Tables 3 and 4 present results for the FLUENT simulations (exit stream temperature and flow rates and exit gas composition). Figures 3 and 4 show the steady state distribution of various gas-phase components within the gasifier.

4. GASIFIER UNCERTAINTY CHARACTERIZATION AND QUANTIFICATION

Although IGCC system has been a topic of research for many years, its commercialization has been limited. Therefore, there is a significant lack of information on the commercial-scale performance of the IGCC system. This uncertainty limits the optimization and performance evaluation of the existing system as well as any improvements to the system. The predication of the cost and performance of mature and commercial-scale technology using preliminary research data can be risky.[25,26] Consequently, there have been efforts to systematically incorporate uncertainty in the process analysis and design optimization steps. Frey and Rubin[27] developed a probabilistic approach for evaluating technology performance and used it to compare two different design alternatives for the IGCC system. They also used this methodology to quantify trade-offs and identify research needs. Other efforts considering uncertainty in the performance analysis of the IGCC system include those in refs 28−32.

The gasifier is an important component of the IGCC system. Operation of the gasifier depends on numerous parameters, some of them not always deterministically known and subject to uncertainty. Another important cause of uncertainty is due to the modeling assumptions incorporated in the system-level IGCC model in ASPEN Plus. Stochastic simulation allows quantification of the impact of variations in the gasifier parameters on its performance. However, for the study to be reliable, it is very critical that the uncertainty is appropriately characterized and quantified. This is especially important for a system such as IGCC where the system level models involve approximations of individual components and where the quality of the models has not been thoroughly verified. This work, therefore, focused on the characterization and quantification of the gasifier uncertainty by considering the approximate and comprehensive models of the gasifier using ASPEN Plus flowsheet and CFD approach, respectively. This information can then be used in the CAPE-OPEN compliant "StochaSim" stochastic simulation

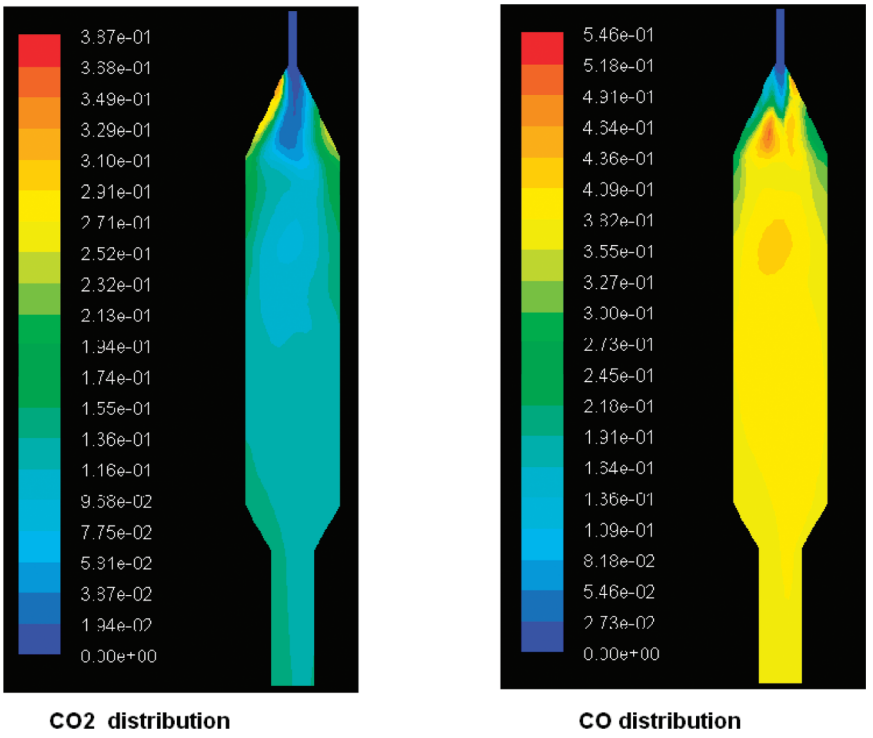

Figure 3. Distribution of CO_2 and CO concentration within the gasifier.

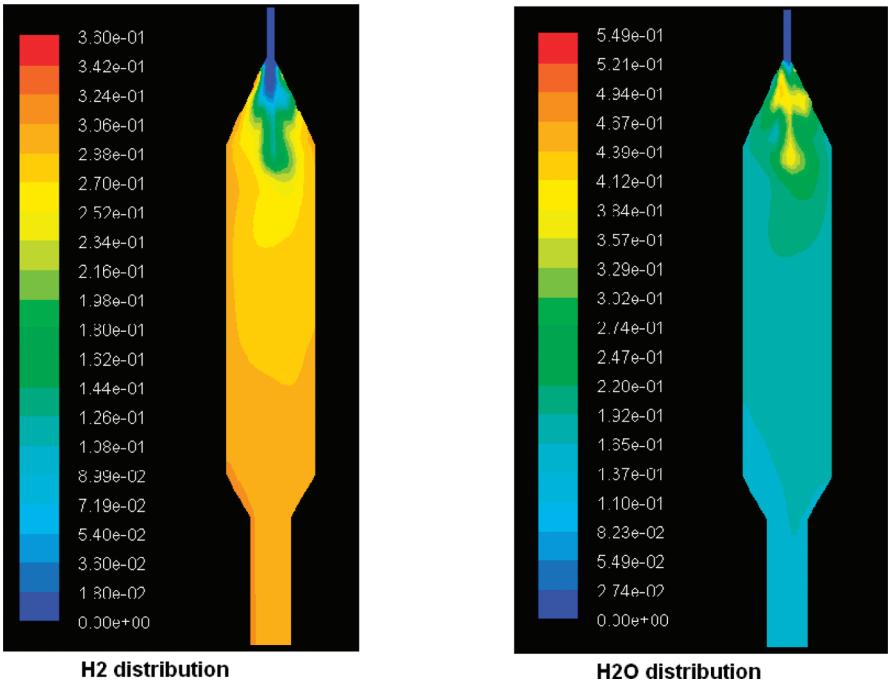

Figure 4. Distribution of H_2 and H2O concentration within the gasifier.

block in ASPEN Plus which enables us to study the effect of uncertainty on the complete IGCC system.

Uncertainty analysis consists of four main steps: (1) characterization and quantification of uncertainty in terms of probability distributions, (2) sampling from these distributions, (3) propagation through the modeling framework, and (4) analysis of results.[32] The first step is of foremost importance and the one on which the validity of the uncertainty analysis is contingent. Characterization refers to the process of representing uncertainty through mathematical expressions to facilitate analysis with mathematical tools.[33] The diverse nature of uncertainty can be specified in terms of different probability distributions. The type of distribution chosen for an uncertain variable reflects the amount of information that is available. It is easier to assume

the upper and lower bounds of uncertain variables, and hence uniform distribution is the first step toward uncertainty quantification. If one can identify the most likely value then triangular distributions can be used. If more data are available, specific properties of distributions are used for characterization. For example, the uniform and log-uniform distributions represent an equal likelihood of a value lying anywhere within a specified range, on either a linear or logarithmic scale, respectively. Further, a normal (Gaussian) distribution reflects a symmetric but varying probability of a parameter value being above or below the mean value. In contrast, log-normal and some triangular distributions are skewed such that there is a higher probability of values lying on one side of the median than the other.

It is quite challenging to quantify and characterize the operational uncertainty of a system. The ideal approach is to compare the simulation results with actual operating data of the system. However, this is often not possible because there are no data or limited operating data available. Moreover, conducting perturbation studies on an actual system to generate such data is not feasible due to the associated risks. The ASPEN Plus flowsheet for the IGCC system modeled the gasifier using a simplified reactor model. The CFD model developed in FLUENT in comparison was much more rigorous and captured the features of a multiphase system. Consequently, the operational details from the CDF model were more realistic than those from the APSEN Plus model. Hence, in the absence of real operating data, this work used the CFD model of the gasifier for the uncertainty characterization. An uncertainty factor was defined as:

$$\text{Uncertainty Factor (UF)} = \text{FLUENT result/ASPEN result} \quad (1)$$

where result refers to any variable in the gasifier operation (such as temperature, exit gas composition). It can therefore be seen that this factor captures the divergence of the system-level ASPEN Plus model results from a more accurate and dedicated CFD model of the gasifier unit. However, to characterize and quantify the gasifier operating uncertainty, it is necessary to utilize multiple data points. Hence, to ensure that the most appropriate distribution is used to represent the operational uncertainty in the gasifier, this work conducted a sampling and simulation study in the FLUENT as well as ASPEN Plus gasifier model. To perform this analysis, the probable uncertain input parameters to the gasifier, including their distribution, were first identified. Later, a selected number of samples for those parameters were generated. The FLUENT and ASPEN Plus models were simulated for each sample. The results for various important gasifier model variables were then compared according to the equation given above to compute the uncertainty factor for the model. The actual values of the UF also allowed the quantification of uncertainty since the type and property of the distribution for the uncertainty factor could be estimated. This general procedure was implemented for the gasifier model uncertainty characterization and quantification. The exact details for the gasifier are presented in the next section.

4.1. Gasifier Results. For the gasifier, 12 different parameters were identified as uncertain for the modeling purpose. The parameters were assumed to vary between ±25% of their base case values. This range of variation was not based on a prior analysis of the IGCC system but rather reflected the typical variation that might be expected in the parameters. The list of the parameters, along with the base case values and the upper and lower bounds, is presented in Table 5. The parameters were sampled using the Monte Carlo sampling technique assuming uniform distribution between the bounds. This work used 15 samples within this range. Although it was expected that the proximate and the ultimate analysis of the coal would be related, the sampling ignored such correlations. Once the samples were generated, the parameters for the ultimate and proximate analysis of the coal were normalized so that the total sum of the percentage compositions for each analysis was 100.

Table 5. Uncertainty Parameter Details

parameter	base value	lower bound	upper bound
slurry water injection rate (kg/s)	12.95	9.712	16.18
coal injection rate (kg/s)	31.52	23.64	39.40
oxidant injection rate (kg/s)	26.38	19.89	32.98
proximate analysis of coal (%)			
fixed carbon	49.72	37.29	62.15
moisture	11.12	8.34	13.90
volatile matter	29.37	22.03	36.71
ash	10.91	8.18	13.36
ultimate analysis of coal (%)			
carbon	71.72	53.79	89.65
hydrogen	5.06	3.79	6.32
nitrogen	1.74	1.30	2.17
oxygen	7.75	5.83	9.69
sulfur	2.82	2.11	3.52

Table 6. Uncertainty Quantification for Exit Gas Mass Flow Rate

fluent value (kg/s)	ASPEN value (kg/s)	UF
70.04	66.55	1.05
66.37	65.67	1.01
70.97	63.05	1.12
71.74	68.86	1.04
68.18	67.68	1.01
70.41	61.62	1.14
53.20	71.60	0.74
72.94	60.08	1.21
70.11	61.82	1.13
70.83	68.90	1.02
71.88	62.87	1.14
62.99	61.25	1.02
64.59	64.81	0.98
69.34	63.55	1.09

For each sample, the FLUENT CFD model and the IGCC system in ASPEN were simulated. The important variables of the gasifier that were used to compute the uncertainty factor were the following: total exit gas mass flow rate, total slag mass flow rate, and otal mass flow rate of different constituents of the exit gas (such as CO and CO_2).

Table 6 gives an example of the calculation of the uncertainty factor for the exit gas mass flow rate. For one sample set, both FLUENT and Aspen Plus simulation results led to output values that were significantly different from the rest of the values. Since this would have skewed the resulting distribution, that sample was ignored and only 14 samples were used for the calculations of the uncertainty factor and its distribution. The values of the

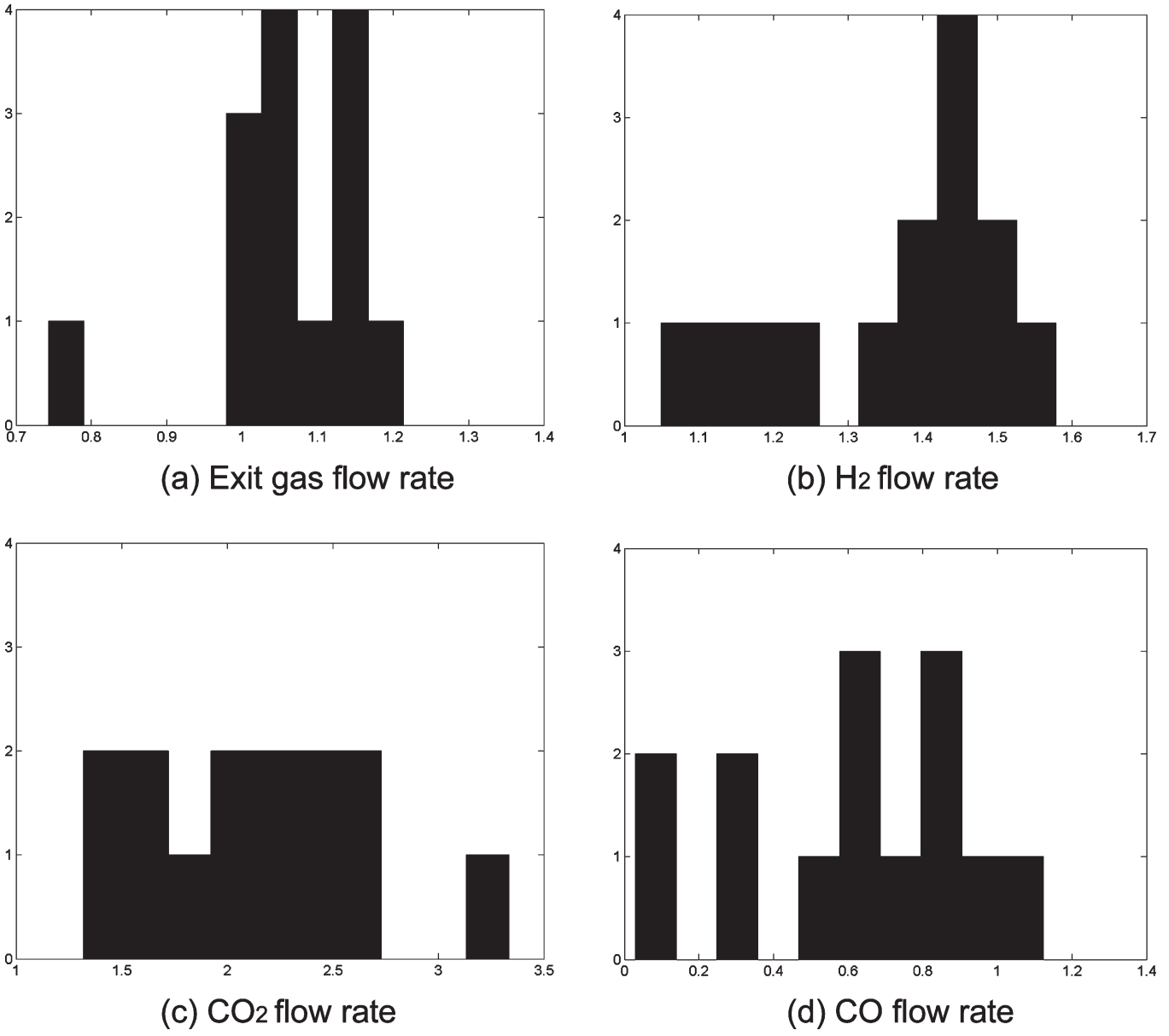

Figure 5. Distribution of uncertainty factors for selected gasifier variables using histograms. *Y*-axis represents the number of instances of a particular value of uncertainty factor among 14 samples.

uncertainty factor were then used to plot the distribution of the uncertainty factor. With a large number of samples, it is possible to use kernel density estimation to determine the probability density function of the uncertainty factor. However, in this case, only 15 samples were used. Hence, the characterization of uncertainty was done by plotting the uniform* distribution (histogram). This distribution can then be used to simulate the stochastic system. The distributions obtained for the important variables of analysis are shown in Figure 5.

5. MULTIOBJECTIVE OPTIMIZATION OF IGCC

The IGCC system is a complex and highly nonlinear system with various parameters that define the overall performance of the system. No single parameter can be the true representative of the system performance, and hence the optimization of the whole system must consider all such representative objectives. Such problems are known as multiobjective problems in optimization literature. Quite often such objectives are conflicting and hence a systematic approach must be employed. This section focuses on the multiobjective optimization of the IGCC flowsheet using the CAPE-OPEN capability of stochastic modeling and the Parameter Space Investigation (PSI) method.[15,34]

5.1. Multiobjective Optimization Approach. Multiobjective problems appear in virtually every field and in a wide variety of contexts. The importance of multiobjective optimization can be seen by the large number of applications presented in the literature. The problems solved vary from designing spacecrafts,[35] aircraft control systems,[36] bridges,[37] and highly accurate focusing systems,[38] to forecasting manpower supplies,[39] managing nuclear waste disposal and storage,[40] allocating water resources,[41] and solving pollution control and management problems.[42] Most of these applications are multiobjective problems of nonlinear nature, which is why we need tools for

Table 7. Sample Parameters for Determination of Pareto Surface for IGCC System

parameter	lower bound	upper bound
gasifier operating temperature (°C)	1182.2	1448.8
gasifier operating pressure (MPa)	5.05	6.17
first water gas shift cooler temperature (°C)	207.22	257.22
second water gas shift cooler temperature (°C)	207.22	257.22
sour gas heater temperature (before combustion) (°C)	207.22	257.22
sulfur condenser 1 temperature (°C)	207.22	257.22
preheating for hydrogenation temperature (°C)	207.22	257.22
condenser for water from hydrogenation heater temperature (°C)	42.22	55.55
Claus gas oxidant heater temperature (°C)	207.22	257.22
tail gas hydrogenation reactor temperature (°C)	207.22	257.22
Claus burner temperature (°C)	1182.2	1448.8

nonlinear programming capable of handling multiple conflicting or incommensurable (e.g., different units) objectives.

The solution of a multiobjective optimization problem is a set of solution alternatives called the Pareto set. For each of these solution alternatives, it is impossible to improve one objective without sacrificing the value of another, relative to some other solution alternatives in the set. There are usually many (infinite in number) Pareto optimal solutions. The collection of these is called the Pareto set. The result of the application of a nonlinear multiobjective technique to a decision problem is the Pareto set for the problem, and it is from this subset of potential solutions that the final, preferred decision is chosen by the decision-makers. The selection of the appropriate method often depends on the optimization problem formulation. In this work, the nondominated (Pareto) surface for the IGCC system was computed for following three important performance measures of the system, constituting the objectives for the system:

- total plant efficiency (based on HHV of coal) (objective 1)
- total CO_2 emissions measured in kg/h (objective 2)
- total SO_x emission measured as volumetric fraction of the total flue gas volumetric flow rate (objective 3)

5.2. Partial Rank Correlation Coefficient Study. To conduct multiobjective optimization, it is important to identify the important parameters in the model that have a significant impact on the system performance. This is however more complicated due to the complex (often nonlinear) interactions within the model. One way of identifying this is to do parametric sensitivity analysis. However, this typically involves perturbing parameters around some specific points. Therefore, this sensitivity is restricted to a local region of operation. This work, therefore, used stochastic analysis[42] based on sampling to obtain partial correlation and partial rank correlation coefficients (PCC and PRCC), thus providing overall sensitivity. PCC corresponds to partial correlation coefficient, and provides a major or unique or unshared contribution of each variable, and explains the unique relationship between two variables that cannot be explained in terms of the relations of these variables with any other variable. PCCs are useful when the model is relatively linear. For nonlinear models, partial rank correlation coefficient (PRCC) is supposed to provide information equivalent to PCC, and hence this work used the PRCC values for the IGCC system. The computation of the PRCCs was carried out through sampling analysis.[43] Initially, candidate model parameters were identified and sampled in the neighborhood of the base case parameter values, and the model was simulated for each sample set. The simulation results along with the parameter samples were used to compute the coefficients. For the analysis to be exhaustive, it was important to cover the complete range of the possible parameter values. Eleven parameters of the IGCC system listed below were identified and used for the PRCC analysis:

- Gasifier operating temperature
- Gasifier operating pressure
- First water gas shift cooler temperature (syngas cooler)
- Second water gas shift cooler temperature (syngas cooler)
- Sour gas heater temperature before combustion (Claus process)
- Sulfur condenser 1 temperature
- Preheating for hydrogenation temperature
- Condenser for water from hydrogenation heater temperature
- Claus gas oxidant heater temperature
- Tail gas hydrogenator reactor temperature
- Claus burner temperature

These parameters were sampled around the base case values given for the basic ASPEN Plus flowsheet. The parameters were uniformly sampled around the mean and 150 samples in the desired region were taken. The parameters with the lower and upper bounds are listed in Table 7. The PRCC values for all the possible pairs between the selected model parameters and the three objectives were computed. The results for the analysis are presented in Table 8. Greater deviation of the PRCC from zero in positive or negative direction indicates a stronger direct or inverse correlation, respectively, between the parameter and the objective. Therefore, the absolute values of PRCCs for each parameter with each of the objectives were summed and the parameters were sorted in the decreasing order of the cumulative PRCC values. However, in addition to the sum of the PRCC values, it was ensured that the selected parameters had some impact on all the three objectives. Therefore, although the first water gas shift cooler temperature had a high cumulative PRCC value, it was not selected since its impact on SO_x emissions is negligible. Using these selection criteria, the following three parameters were identifies as the ones with a significant impact on the objectives of the IGCC system: gasifier operating temperature, gasifier operating pressure, and Claus burner temperature. These parameters were used to analyze results of multiobjective optimization and are referred to as variables 1, 2 and 3, respectively, in the subsequent text.

5.3. Nondominated Set for IGCC System. Although constraint-based or preference-based methods give a good estimate of the Pareto surface, they require the use of gradient-based techniques to determine the surface. However, for the given

Table 8. PRCC Results for the IGCC System

parameter	efficiency	CO_2 emission (kg/h)	SO_x emission (volume fraction)
gasifier operating temperature (°C)	0.999	−0.861	0.925
gasifier operating pressure (MPa)	−0.124	0.513	0.024
first water gas shift cooler temperature (°C)	0.928	0.936	−0.001
second water gas shift cooler temperature (°C)	−0.059	0.015	−0.02
sour gas heater temperature (before combustion) (°C)	0.019	0.0006	−0.046
sulfur condenser 1 temperature (°C)	−0.025	−0.015	−0.063
preheating for hydrogenation temperature (°C)	−0.031	0.032	−0.08
condenser for water from hydrogenation heater temperature (°C)	−0.063	−0.011	−0.016
Claus gas oxidant heater temperature (°C)	−0.052	0.041	0.046
tail gas hydrogenation reactor temperature (°C)	−0.089	0.023	−0.068
Claus burner temperature (°C)	0.352	0.059	0.692

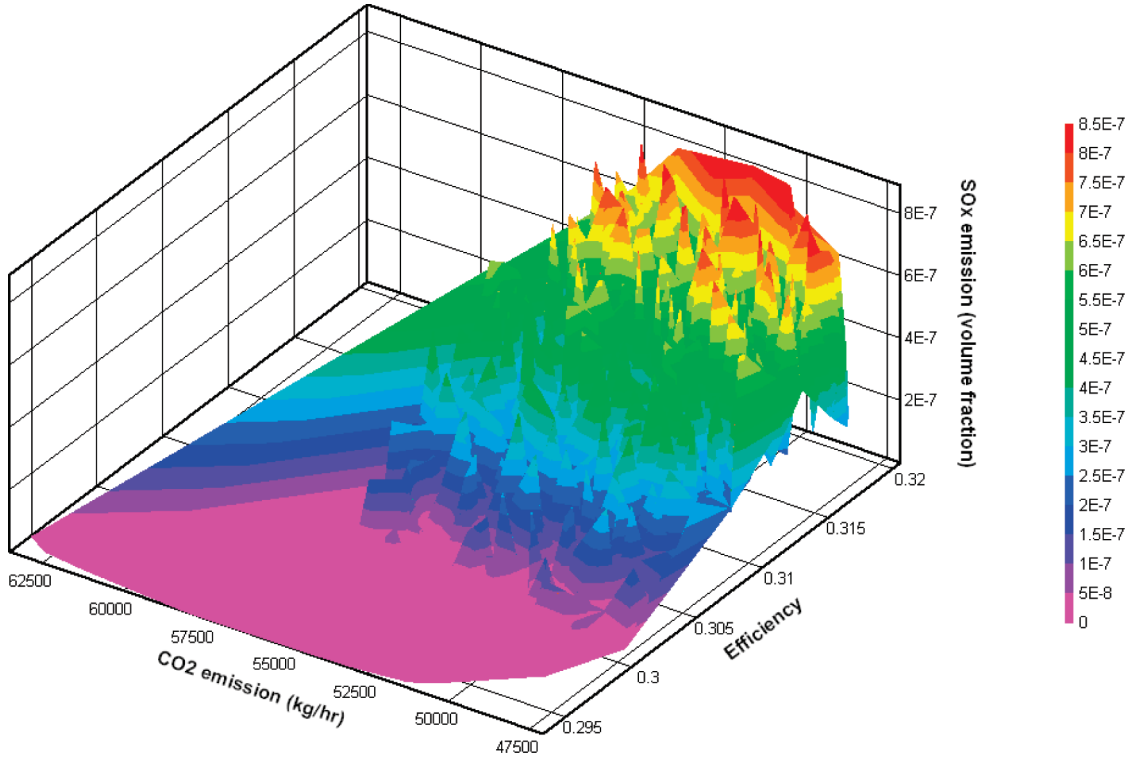

Figure 6. 3-D feasible region and objective function contours for IGCC system.

system, it was observed that the feasible surface is nonconvex (explained later in the section). This made the use of the previously mentioned techniques very difficult. No-preference-based methods can successfully tackle such problems and hence were used in this case. The "No-preference-based methods" include compromise programming,[44,45] Multiobjective Proximal Bundle (MPB),[46] and feasibility-based methods, such as the Parameter Space Investigation (PSI) methods,[47] and focus on generating a feasible solution or all the feasible solutions instead of the Pareto set (the best feasible solutions).[34] In PSI methods, the continuous decision space is first uniformly discretized using the Monte Carlo sampling technique; next a solution is checked with the constraints. If one of the constraints is not satisfied, the solution is eliminated. This is carried out for all the points in the discretized decision space and only feasible solutions are retained. Therefore, a discretized approximation of the feasible objective region, instead of the Pareto set, is retained by the PSI method. The solutions of this feasibility-based method cover the whole feasible objective region rather than covering only the optimal solutions in the Pareto set. Because most of the feasible solutions are not Pareto optimal, a relatively small number of the nondominated (relatively better, but not necessarily Pareto optimal) solutions must be extracted from the whole feasible solution set to formulate an approximate representation of the Pareto set for feasibility-based methods. A large number of runs must be used to obtain maximum feasible solutions to ensure that a certain number of nondominated solutions can be extracted from them to ensure an accurate representation of the Pareto set. Therefore, the computational efficiency is low for this feasibility-based method. This work though used the PSI method along with Hammersley Sequence Sampling[48] to circumvent this problem as it can handle the nonconvex trade-off surface, as observed here.

As mentioned before, the multiobjective optimization was done with respect to the eleven model parameters (decision variables) and three objectives listed before. The feasible surface

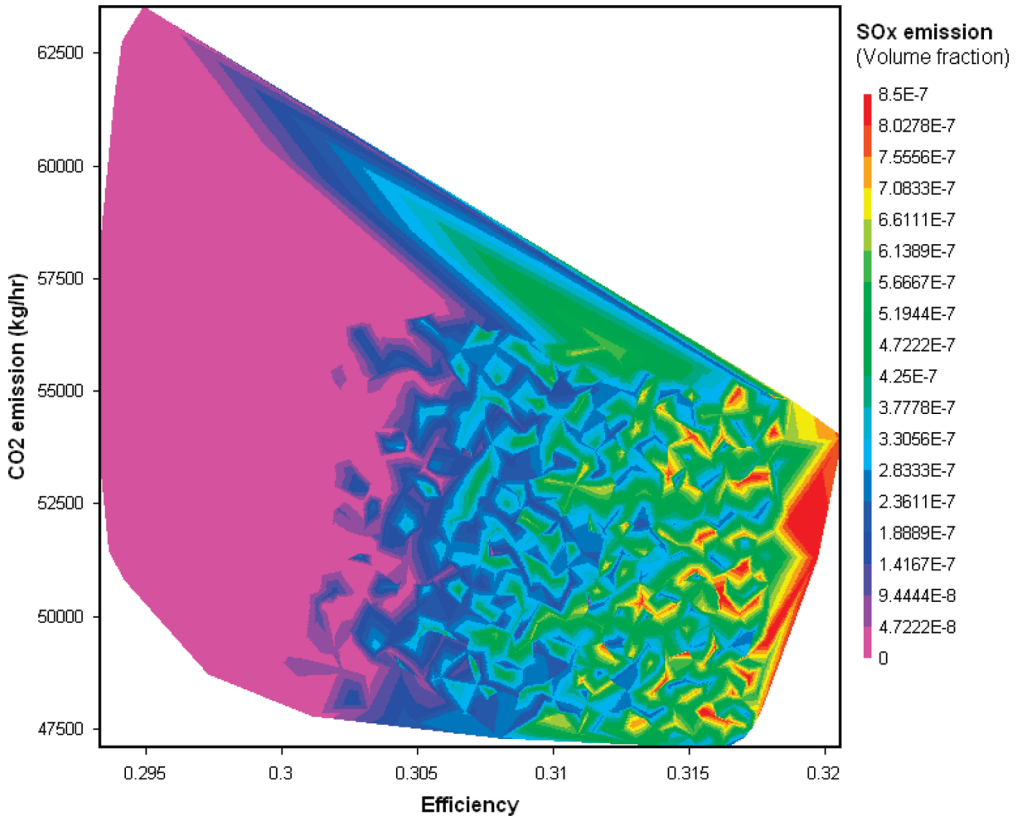

Figure 7. 2-D feasible region and objective function contours for IGCC system.

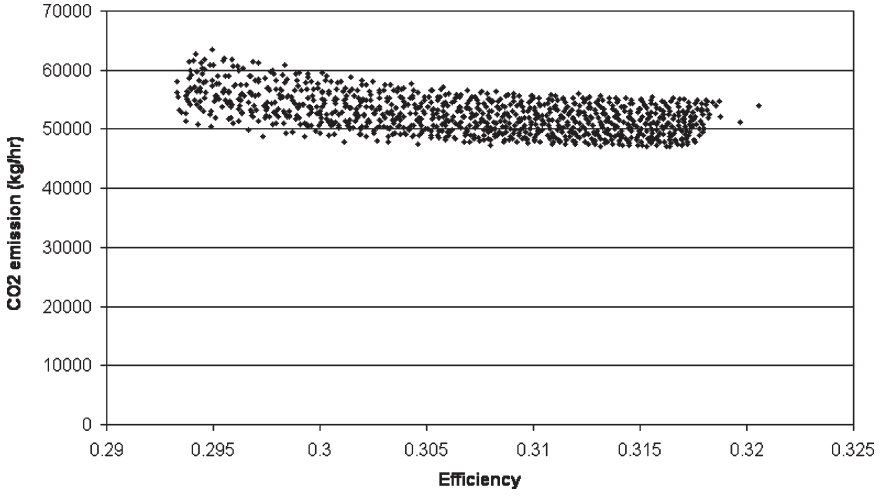

Figure 8. Feasible solutions: CO_2 emissions versus efficiency.

was generated by using 1000 samples for the model parameters and using stochastic simulation capability to compute the objective values. Figure 6 and Figure 7 show the feasible surface for the system and the values of the three objective functions for the simulations in 3-dimensional and 2-dimensional space, respectively. Here, the contours of one of the objectives (SO_x) are plotted with respect to the values of the other two objectives for the 1000 samples. Please note that CO_2 emissions were measured in kg/h while the SO_x emissions were measured in volumetric fraction of the total exit gas volume. Figures 8 and 9 present emissions versus efficiency plots for the feasible space. It can be seen that there are a number of solutions having the same efficiency ranging from low to high emissions. From the figures, it is clearly evident that the trade-off surface was highly nonconvex. One could observe multiple peaks and valleys in terms of one of the objectives when the other two objectives were varied. This justified the use of PSI method to generate the approximate Pareto surface.

To generate the surface, the results for the 1000 simulations were inspected visually. In addition to this, some simple data processing and manipulation techniques were used to get an idea about the approximate Pareto surface for the problem. Table 9

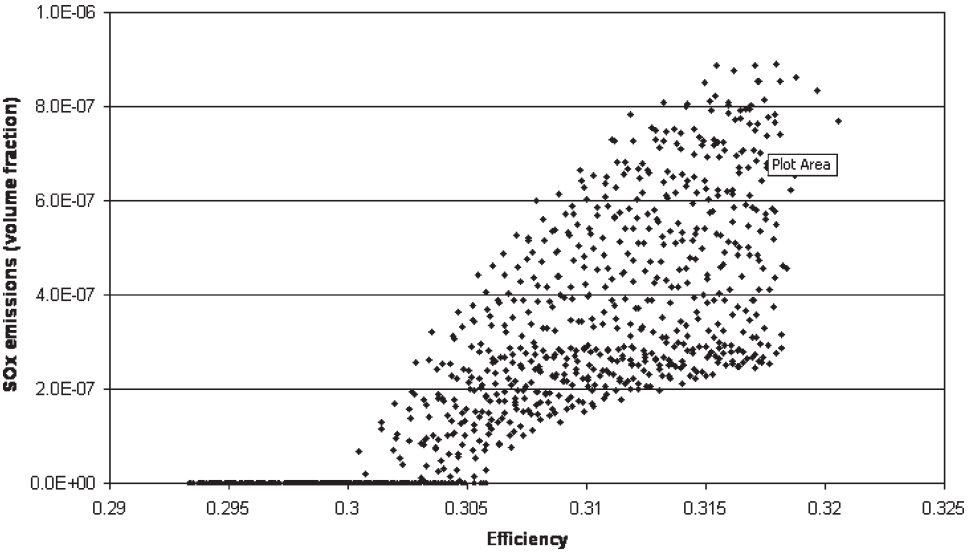

Figure 9. Feasible Solutions: SO_x emissions versus efficiency.

Table 9. Range of Values for the Objectives

	efficiency	CO_2 emission (kg/h)	SO_x emission (volume fraction)
minimum	0.29332	47089.35	0
maximum	0.32057	63524.19	8.9×10^{-7}
percentage variation	8.50	11.72	−

shows the minimum and maximum values of the three objectives among the 1000 samples while the Pareto surface for the system is shown in Table 10. The points on the Pareto surface are plotted in Figure 10 (the points are represented in the Figure as A-B-C-D-E-F). From the table and the trade-off surface shown in Figure 10, it is clear that very low SO_x emissions were often accompanied by low overall efficiency. Hence the two objectives were highly conflicting. The case of CO_2 emission, however, did not show any such trend. In general though, it was observed that lower emissions of CO_2 were often associated with lower SO_x emission but also lower efficiency. The trend though was not as strong as that between SO_x and efficiency. The points listed in Table 10 represent the approximate nondominated set. Because the set had been determined through heuristic methods, it is possible that a few points have been eliminated. However, given the nature of the trade-off surface, it will be very difficult to determine the complete Pareto surface. The values of the model parameters (decision variables) for the identified points on the nondominated set are presented in Table 11.

The deterministic Pareto surface provides the trade-offs among various objectives. However, we have seen in the preceding section that the Gibbs free energy model has uncertainties as compared to rigorous CFD model of gasifier. These uncertainties are characterized in terms of uniform* distributions. Therefore, it is important to see how these uncertainties affect the Pareto surface. To carry out the multiobjective optimization in the face of uncertainties, one has to use stochastic modeling to obtain the expected values of objectives and constraints. These values are then used by the multiobjective programming (MOP) optimizer (stochastic modeling) to find the values of decision variables that can optimize the expected values of objective function. This involves two sampling loops since we use the PSI method with

Table 10. Pareto Surface for the IGCC System

number	point on Pareto surface (Figure 8)	efficiency	CO_2 emission (kg/h)	SO_x emission (volume fraction)
1	E	0.30111	47759.79	0
2	D	0.30578	53001.0	0
3	F	0.31533	47089.35	3.10×10^{-7}
4	C	0.32057	53956.83	7.68×10^{-7}
5	B	0.31757	47827.74	7.39×10^{-7}
6	A	0.31641	47093.88	2.48×10^{-7}

Hammersley sequence sampling. We developed a new CAPE-OPEN block called STOCHA2 that uses two sampling loops to obtain feasible multiobjective optimization surface under uncertainty. Table 12 shows the feasible surface and corresponding decision variables. It must be noted that feasible region for stochastic system was different than the feasible region for the deterministic system shown in Figures 6 and 7. The plots showing the feasible region for the stochastic system are not included here in the interest of space. It can be seen that the feasible surface narrowed significantly when uncertainties were considered as compared to the deterministic surface. The decision variable range is narrowed significantly too.

6. CONCLUSION

Integrated Gasification Combined Cycle (IGCC) system using coal gasification promises to be one of the sustainable energy alternatives for the future. The operations of the IGCC system, however, are impacted by the presence of uncertainty, particularly by uncertainties in the gasifier operation. This focus of this work was the uncertainty analysis and quantification of the IGCC system and its multiobjective optimization in the presence of uncertainty. Toward that objective, the work first developed a computational fluid dynamics model of a single-stage downflow coal gasifier using FLUENT. This provided a tool to accurately understand the operations of the coal gasifier. The results of the CFD simulation in the presence of uncertainty were compared with the results from an ASPEN Plus model. This enabled the

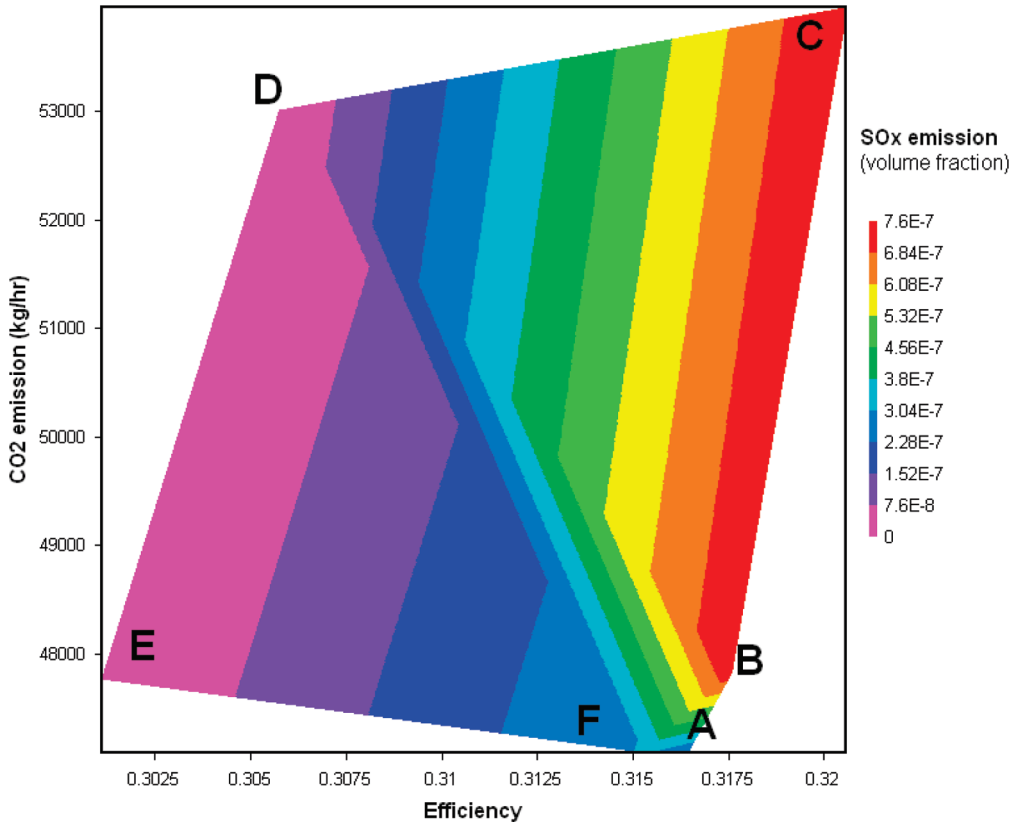

Figure 10. Pareto Surface and Points for IGCC System.

Table 11. Decision Variable Values for the Non-Dominated Set

number	point on Pareto surface (Figure 8)	gasifier operating temperature (°C)	gasifier operating pressure (kPa)	Claus burner temperature (°C)
1	E	1257.61	5109.33	1229.78
2	D	1302.63	5737.81	1185.71
3	F	1420.65	5237.88	1264.02
4	C	1448.35	5334.57	1421.30
5	B	1447.02	6108.08	1375.32
6	A	1435.03	5422.47	1227.88

Table 12. Stochastic Non-Dominated Set for the IGCC System

	objectives			decision variables		
design	efficiency	CO_2 emission (kg/h)	SO_x emission (volume fraction)	gasifier operatingtemperature (°C)	gasifier operatingpressure (kPa)	Claus burnertemperature (°C)
1	0.319	5.193×10^4	0.1767×10^{-5}	1448.8	5612.3	1439.4
2	0.306	4.486×10^4	0.8822×10^{-6}	1447.2	5895	1430.5
3	0.306	4.762×10^4	0.8183×10^{-6}	1445.5	5336.5	1421.1

quantification of the uncertainty factors and allowed the characterization of the uncertainty. The results showed that the uncertainty factors vary substantially. To conduct multiobjective optimization of the IGCC system, a partial rank correlation coefficient analysis was first conducted to determine the important variables affecting the system performance. The important performance indicators for the system were also identified. Because the feasible region of the IGCC system operation was highly nonconvex, gradient-based methods could not be used to solve the optimization problem. Hence, the Parameter Space Investigation (PSI) approach using stochastic simulations was used to determine the nondominated set for the IGCC system. The results showed that lower SO_x and CO_2 emissions typically lead to lower efficiency. It was also observed that uncertainty has a significant impact on the Pareto surface.

AUTHOR INFORMATION

Corresponding Author

*Tel.: +1-630-886-3047. E-mail: urmila@vri-custom.org.

Present Addresses

[†]Current affiliation: Energy Biosciences Institute, Department of Agricultural and Biological Engineering, University of Illinois at Urbana−Champaign.

■ ACKNOWLEDGMENT

This research work has been funded by the National Energy Technology Laboratory (NETL) under contract RDS SUBTASK 41817.312.01.06.

■ REFERENCES

(1) Weiber, P. R.; Halow, J. S. Advanced IGCC power systems for the United States. *Energy Prog.* **1987**, *7* (2), 119.

(2) Schafer, W.; Trondt, M.; Langhoff, J.; Konkol, W.; Hibbel, J. Coal gasification for synthesis and IGCC processes: Results of the development of Texaco coal gasification by Ruhrkohle AG/Ruhrchemie AG. *Fuel Process. Technol.* **1988**, *17* (3), 221.

(3) Joshi, M. M.; Lee, S. Integrated gasification combined cycle - A review of IGCC technology. *Energy Sources* **1996**, *18* (5), 537.

(4) Pruschek, R.; Oeljeklaus, G.; Haupt, G.; Zimmermann, G.; Jansen, D.; Ribberink, J. S. The role of IGCC in CO_2 abatement. *Energy Convers. Manage.* **1997**, *38* (1), S153.

(5) Ratafia-Brown, J.; Manfredo, L.; Hoffmann, J.; Ramezan, M. *Major Environmental Aspects of Gasification-Based Power Generation Technologies*; Final report, prepared by Science Applications International Corporation for the U.S. Department of Energy: Washington DC, December 2002.

(6) Holt, N. Operation experience and improvement opportunities for coal-based IGCC plants. *Mater. High Temp.* **2003**, *20*, 1.

(7) Bissett Larry, A.; Strickland Larry, D. Analysis of a fixed-bed gasifier IGCC configuration. *Ind. Eng. Chem. Res.* **1991**, *30*, 170.

(8) Bridgwater, A. V. The technical and economic feasibility of biomass gasification for power generation. *Fuel* **1995**, *74*, 631.

(9) Ordorica-Garcia, G.; Douglas, P.; Croiset, E.; Zheng, L. Techno-economic evaluation of IGCC power plants for CO_2 avoidance. *Energy Convers. Manage.* **2006**, *47* (15−16), 2250.

(10) Jin, H.; Ishida, M. New advanced IGCC power plant with chemical-looping combustion. In *Proceedings of the International Conference on Thermodynamic Analysis and Improvement of Energy Systems*, Beijing, China, June 1997; pp 548−553.

(11) Rhodes, J. S.; Keith, D. W. Engineering economic analysis of biomass IGCC with carbon capture and storage. *Biomass Bioenergy* **2005**, *29*, 440.

(12) Shinada, O.; Yamada, A.; Koyama, Y. The development of advanced energy technologies in Japan: IGCC - a key technology for the 21st century. *Energy Convers. Manage.* **2002**, *43* (9−12), 1221.

(13) Kaldis, S. P.; Skodras, G.; Sakellaropoulos, G. P. Energy and capital cost analysis of CO_2 capture in coal IGCC processes via gas separation membranes. *Fuel Process. Technol.* **2004**, *85* (5), 337.

(14) Descamps, C.; Bouallou, C.; Kanniche, M. Efficiency of an integrated gasification combined cycle (IGCC) power plant including CO_2 removal. *Energy* **2008**, *33*, 874.

(15) Subramanyan, K.; Diwekar, U.; Zitney, S. Stochastic modeling and multiobjective optimization for the APECS system. *Comp. Chem. Eng.* **2010**, under Review.

(16) USDOE/NETL. *Model Documentation: IGCC with GE Energy Gasifier and CO_2 Capture*; Technical Report /NETL-401/042606; United States Department of Energy, National Energy Technology Laboratory: Morgantown, VA, 2007.

(17) Chen, C.; Horio, M.; Kojima, T. Numerical simulation of entrained flow coal gasifiers. Part I: Modeling of coal gasification in an entrained flow gasifier. *Chem. Eng. Sci.* **2000**, *55*, 3867.

(18) Watanabe, H.; Otaka, M. Numerical simulation of coal gasification in entrained flow coal gasifier. *Fuel* **2006**, *85* (12−13), 1935.

(19) Govind, R.; Shah, J. Modeling and simulation of an entrained flow coal gasifier. *AIChE J.* **1984**, *30*, 79.

(20) Vicente, W.; Ochoa, S.; Aguillon, J.; Barrios, E. An eulerian model for the simulation of an entrained flow coal gasifier. *Appl. Thermal Eng.* **2003**, *23* (15), 1993.

(21) Shi, S.-P.; Zitney, S. E.; Shahnam, M.; Syamlal, M.; Rogers, W. A. Modelling coal gasification with CFD and discrete phase method. *J. Energy Inst.* **2006**, *79*, 217.

(22) Bockelie, M. J.; Holt, N. CFD modeling for entrained flow gasifiers. In *Proceedings of the Gasification Technologies Conference*, 2002.

(23) Bockelie, M. J.; Denison, M. K.; Chen, Z.; Linjewile, T.; Senior, C. L.; Sarofim, A. F. CFD modeling for entrained flow gasifiers in vision 21 systems. In *International Pittsburgh Coal Conference*, 2002.

(24) Bockelie, M. J.; Denison, M. K.; Shim, H.; Senior, C. L.;, Sarofim, A. F. CFD modeling for entrained flow gasifiers. In *ACERC Annual Conference*, 2005.

(25) Hess, R. W.; Myers, C. W. *Assessing Initial Cost Growth and Subsequent Long Term Cost Improvement in Coal-to-SBG Processes*; Report No. GRI-89/0129; Gas Research Institute: Chicago, IL, June 1989.

(26) Merrow, E. W.; Phillips, K. E.; Myers, C. W. *Understanding Cost Growth and Performance Shortfalls in Pioneer Process Plants*; Report No. R-2569-DOE; Rand Corporation: Santa Monica, CA, September 1981.

(27) Frey, H. C.; Rubin, E. S. Evaluation of advanced coal gasification combined-cycle systems under uncertainty. *Ind. Eng. Chem. Res.* **1992**, *31*, 1299.

(28) Frey, H. C.; Rubin, E. S.; Diwekar, U. M. Modeling uncertainties in advanced technologies: Application to a coal gasification system with hot-gas cleanup. *Energy* **1994**, *19*, 449.

(29) Zu, Y.; Frey, H. C. Uncertainty analysis of integrated gasification combined cycle systems based on Frame 7H versus 7F gas turbines. *J. Air Waste Manage. Assoc.* **2006**, *56*, 1649.

(30) Chen, C.; Rubin, E. S. CO_2 control technology effects on IGCC plant performance and cost. *Energy Policy* **2009**, *37*, 915.

(31) Jin, H.; Larson, E. D.; Celik, F. E. Performance and cost analysis of future, commercially mature gasification-based electric power generation from switchgrass. *Biofuels, Bioprod. Biorefin.* **2009**, *3*, 142.

(32) Diwekar, U. M.; Rubin, E. S.; Frey, H. C. Optimal design of advanced power systems under uncertainty. *Energy Convers. Manage.* **1997**, *38* (15−17), 1725.

(33) Subramanyan, K.; Diwekar, U. M.; Goyal, A. Multi-objective optimization of hybrid fuel cell power system under uncertainty. *J. Power Sources* **2004**, *132*, 99.

(34) Diwekar, U. M. *Introduction to Applied Optimization*, 2nd ed.; Springer: New York, 2008.

(35) Sobol, I. M. A global search for multicriterial problems. In *Multiple Criteria Decision Making: Proceedings of the Ninth International Conference*; Springer-Verlag: New York, 1992; pp 401−412.

(36) Schy, A. A.; Giesy, D. P. Multicriteria optimization methods for design of aircraft control systems. In *Multicriteria Optimization in Engineering and in the Sciences*; Plenum Press: New York, 1988; pp 225−262.

(37) Ohkubo, S.; Dissanayake, P. B. R.; Taniwaki, K. An approach to multicriteria fuzzy optimization of a prestressed concrete bridge system considering cost and aesthetic feeling. *Struct. Optim.* **1998**, *15*, 132.

(38) Eschenauer, H. A. Multicriteria optimization techniques for highly accurate focusing systems. In *Multicriteria Optimization in Engineering and in the Sciences*; Plenum Press: New York, 1988; pp 309−352.

(39) Silverman, J.; Steuer, R. E.; Whisman, A. W. A multi-period, multiple criteria optimization system for manpower planning. *Eur. J. Oper. Res.* **1988**, *34*, 160.

(40) Ferreira, P. A. V.; Machado, M. E. S. Solving multiple-objective problems in the objective space. *J. Optim. Theory Appl.* **1996**, *89*, 659–680.

(41) Fu, Y.; Diwekar, U.; Young, D.; Cabezas, H. Process design for environment: A multiobjective framework under uncertainty. *J. Clean Prod. Processes* **2000**, *2*, 92.

(42) Fu, Y.; Diwekar, U. Cost effective environmental management for utilities. *Adv. Environ. Res.* **2004**, *8*, 173.

(43) Diwekar, U. M.; Rubin, E. S. Stochastic modeling of chemical processes. *Comput. Chem. Eng.* **1991**, *15*, 105.
(44) Zeleny, M. *Linear Multi-Objective Programming: Lecture Notes in Economics and Mathematical Systems*; Springer-Verlag: Heidelberg, 1974.
(45) Yu, P. L. *Multiple-Criteria Decision Making Concepts, Techniques, and Extensions*; Plenum Press: New York, 1985.
(46) Miettinen, K. M. *Nonlinear Multi-Objective Optimization*; Kluwer Academic Publishers; Boston, MA, 1999.
(47) Osyczka, A. *Multicriteria Optimization in Engineering with FORTRAN Programs*; Ellis Horwood Limited: Boston, MA, 1984.
(48) Kalagnanam, J. R.; Diwekar, U. An efficient sampling technique for off-line quality control. *Technometrics* **1997**, *39*, 308.